Eternal annihilations: New constraints on long-lived particles from big-bang nucleosynthesis

Joshua A. Frieman
NASA/Fermilab Astrophysics Center, Fermi National Accelerator Laboratory, Batavia, Illinois 60510-0500

Edward W. Kolb and Michael S. Turner
NASA/Fermilab Astrophysics Center, Fermi National Accelerator Laboratory, Batavia, Illinois 60510-0500
and Department of Astronomy and Astrophysics, Enrico Fermi Institute, The University of Chicago, Chicago, Illinois 60637-1433

(Received 11 September 1989)

In the early Universe, the relative abundance of a massive weakly interacting particle species "freezes out" when the annihilation rate becomes less than the expansion rate. Although ineffective in reducing the total number of the species, occasional annihilations still occur after freeze-out. The residual annihilations of massive particles (10 MeV $\lesssim m_X \lesssim 1$ GeV) after primordial nucleosynthesis can strongly alter the light-element abundances through photodissociation. For particles with typical weak-interaction cross sections and lifetimes $\tau_X \gtrsim 5\times 10^6$ sec, we find that the mass range $m_X \lesssim 1$ GeV is ruled out, independent of how they subsequently decay.

I. INTRODUCTION

The standard big-bang cosmology provides important constraints upon the properties of massive particles. In particular, weakly interacting particles with masses in the range of about $m_X = 100$ eV to 2 GeV must be unstable.[1] Otherwise, their present energy density would result in $\Omega_X h^2 > 1$,[2] leading to a Universe that is younger than 10 Gyr when the temperature of the microwave background is 2.7 K. Furthermore, if they decay into photons or electrons, unstable particles with masses greater than a few MeV can cause photofission of the primordially produced light nuclei,[3] upsetting the agreement between big-bang nucleosynthesis and the observed element abundances. For example, for radiatively decaying neutrinos with mass between 10 MeV and 1 GeV, the lifetime must be[4] less than about 10^4 sec to avoid an overabundance of ^{3}He. However, there are a number of extensions of the standard electroweak model in which massive, unstable particles do not decay electromagnetically, but through other "invisible" channels. For example, in Majoron models,[5] a heavy neutrino may decay to a light neutrino and a Majoron.[6] (Similarly, in supergravity models, the gravitino can decay primarily to a sneutrino-neutrino pair.[7]) In such cases, the usual photofission bounds upon the lifetimes do not apply.

In this paper, we consider a different, less model-dependent constraint on massive long-lived particles, also arising from big-bang nucleosynthesis. Although the *decay products* of such particles may be cosmologically benign, their *annihilation products* must include $e^{\pm}$ and γ's if they are massive enough and couple to the weak current. According to the standard lore, this source of destructive high-energy photons may be neglected because annihilations typically freeze out at a temperature $T_F \sim m_X/20$. For particle masses in the "dangerous" range, $m_X \gtrsim$ a few MeV, freeze-out occurs well before the light elements first become vulnerable to photodissociation, at $T_{\rm dis} \sim$ a few keV. By this late epoch, any photons and electrons generated before freeze-out have harmlessly thermalized. However, after freeze-out, occasional annihilations still take place. Although rare on the expansion time scale, these residual annihilations continue to produce high-energy photons well after nucleosynthesis ends, thereby placing the survival of the light nuclei in jeopardy.

We explore the consequences of these "eternal" annihilations below by calculating the residual annihilation rate, the resulting high-energy photon spectrum, and the corresponding photofission yields. As an example, we derive constraints specifically for Dirac neutrinos, but our results can be applied to any weakly interacting massive particle. The effects of the annihilation of more massive *stable* cold-dark-matter candidates, $m_X \gtrsim$ a few GeV, on the light elements have been considered elsewhere;[8] in that case, hadronic annihilation products dominate, but the net impact on light-element abundances is marginal. Here we consider lighter particles, where the effects of photofission are more pronounced.

II. PARTICLE ANNIHILATIONS AND THE PHOTON SPECTRUM

Consider the annihilations of particle X. Its number density n_X evolves according to the Boltzmann equation[9]

$$\dot{n}_X + 3Hn_X = -\langle \sigma_A |v| \rangle [n_X^2 - (n_X^{\rm eq})^2] , \quad (1)$$

where $\langle \sigma_A |v| \rangle$ is the thermally averaged annihilation cross section, H is the Hubble parameter, $n_X^{\rm eq}(T)$ is the equilibrium number density at temperature T, and an overdot denotes a time derivative. As usual, it is convenient to scale the number density to the entropy density s by defining a new dependent variable $Y_X \equiv n_X/s$. Well before freeze-out, $t \ll t_F$, the annihilation rate $\Gamma_A = n_X \langle \sigma_A |v| \rangle$ is faster than the expansion rate,

$\Gamma_A \gg H$, and the X abundance is kept at its thermal-equilibrium value, $n_X = n_X^{\rm eq}$. We are interested in the epoch long after freeze-out, $t \gg t_F$ (or $T \ll m_X$), when $n_X \gg n_X^{\rm eq}$ and $Y_X \simeq Y_\infty$ has ceased to decrease significantly. In this era, we can ignore X pair creation and consider only annihilation processes. Equation (1) becomes

$$\dot{Y}_X = -\langle \sigma_A |v| \rangle Y_\infty^2 s \ . \tag{2}$$

For a wide variety of particles, we can parametrize the annihilation cross section by

$$\langle \sigma_A |v| \rangle = \sigma_0 \left[\frac{T}{m_X} \right]^n . \tag{3}$$

Here, we have assumed that either s-wave ($n=0$) or p-wave ($n=1$) annihilations dominate; it is straightforward to generalize to the case where both contribute. Characterizing the freeze-out epoch by $x_F \equiv m_X/T_F$ (typically, $x_F \simeq 15$ to 20), the final X abundance is well approximated during the radiation-dominated era by[9]

$$Y_\infty = \frac{5x_F^{n+1}}{[g_{*S}(T_F)/g_*^{1/2}(T_F)] m_{\rm Pl} m_X \sigma_0} \ . \tag{4}$$

Here, $g_*(T_F)$ counts the total number of effectively massless degrees of freedom at freeze-out contributing to the radiation energy density, $\rho_R(T_F) = (\pi^2/30) g_*(T_F) T_F^4$, and $g_{*S}(T_F)$ counts the number of effectively massless degrees of freedom at freeze-out contributing to the entropy density, $s(T_F) = (2\pi^2/45) g_{*S}(T_F) T_F^3$. To get a feel for the importance of annihilations at late times, consider the number of annihilations that occur per comoving volume in a Hubble time: From Eqs. (2)–(4), we find

$$N_A \equiv \frac{|\dot{Y}_X|}{H} \simeq Y_\infty \left[\frac{T}{T_F} \right]^{1+n} . \tag{5}$$

Thus, a fraction $(T/T_F)^{1+n}$ of the relic X particles per comoving volume annihilate each expansion time.

The high-energy $e^\pm$ and γ products of these annihilations initiate electromagnetic cascades with a characteristic spectrum. The most energetic photons in the shower lose energy predominantly by e^+e^- pair production off thermal background photons (double-γ pair production). The resulting high-energy electrons in turn produce secondary energetic γ's by inverse Compton scattering off background photons. At lower energies, photons are degraded mainly by Compton scattering and, to a much lesser extent, photodissociation. The critical energy, above which double-γ pair production dominates over Compton scattering, is given by

$$E_{\rm max}(T) = 2e \frac{m_e^2}{25T} = 0.02e \frac{\rm MeV^2}{kT} \ , \tag{6}$$

where $0.5 \le e \le 1$ is an uncertainty factor which encompasses the various estimates which have appeared in the literature.[8,10,11] In Eq. (6), we have dropped the slight logarithmic dependence of $E_{\rm max}$ on the baryon density $\Omega_B h^2$.

Since double-photon pair production is so efficient, the shower spectrum is essentially cut off at $E \ge E_{\rm max}$. Consequently, photodissociation cannot commence until $E_{\rm max}$ grows larger than the photofission thresholds of the light elements. As the Universe cools, progressively more tightly bound nuclei become vulnerable. When the photons drop below the pair-production threshold, they are found to have the approximate spectrum[12]

$$\xi_\gamma(E) = \begin{cases} B m_X E^{-3/2} E_{\rm max}^{-1/2}, & 0 < E < E_{\rm max} \ , \\ 0, & E > E_{\rm max} \ , \end{cases} \tag{7}$$

where $\xi_\gamma(E)dE$ is the number of shower photons in the energy range $(E, E+dE)$ produced per annihilation, and B is the total branching ratio to $e^\pm$ and γ. (For our purposes, showers initiated by high-energy electrons are essentially identical to those initiated by photons.[8])

The single-annihilation pair-production spectrum of Eq. (7) subsequently evolves due to Compton scattering. We define

$$f_\gamma(E)dE \equiv \frac{1}{s} \left[\frac{dn_\gamma(E)}{dE} \right] dE \tag{8}$$

as the number density of cascade photons in the energy range $(E, E+dE)$, normalized to the entropy density. Then the spectrum evolves according to

$$\dot{f}_\gamma(E) = -\dot{Y}_X \xi_\gamma(E) - f_\gamma(E) Y_e s \sigma_C(E) \ , \tag{9}$$

where the first term on the right-hand side (RHS) is the source due to annihilations and the second term is the sink due to Compton scattering. Here, the electron fraction is

$$Y_e = \frac{n_e}{s} \simeq 0.9 \frac{n_B}{s} = 3.4 \times 10^{-9} (\Omega_B h^2) \tag{10}$$

and the Compton cross section is approximately

$$\sigma_C(E) = \frac{\pi\alpha^2}{m_e^2} \left[\frac{m_e}{2E} \right] [1 + 2\ln(2E/m_e)] \tag{11}$$

for $E_\gamma \gg m_e$. For the energy and temperature range of interest, Eq. (9) rapidly (compared to H^{-1}) approaches its fixed-point solution:[11]

$$f_\gamma(E) = \frac{\xi_\gamma(E) \langle \sigma_A |v| \rangle Y_\infty^2}{Y_e \sigma_C(E)} \ . \tag{12}$$

This is the approximate photon distribution from residual annihilations.

Combining Eqs. (3), (4), (7), (11), and (12), we find the photon distribution at the epoch of photodissociation:

$$f_\gamma(E,T) = \frac{8.4 \times 10^{-14}}{\sqrt{e}\, \Omega_B h^2} \frac{g_*(T_F)}{g_{*S}^2(T_F)} \frac{B x_F^{2n+2}}{(\sigma_0/10^{-38}\ {\rm cm}^2) m_X^{n+1}} \times \frac{T^{n+1/2} E^{-1/2}}{1 + 2\ln(2E/m_e)} \ , \tag{13}$$

for $E < E_{\rm max}$. This analytic estimate agrees well with numerical solutions of the coupled Boltzmann equations for the photon spectrum resulting from a monoenergetic injection source.[10]

III. PHOTODESTRUCTION

We consider the photodissociation and photoproduction of element i, with abundance relative to the entropy (*not* mass fraction) $Y_i = n_i/s$ ($i = {}^4$He, ^{3}H+^{3}He, D, etc.). The destruction and production rates are given by

$$\dot{Y}_i = -Y_i s \sum_{j\neq i} \int_{Q_{i\to j}}^{E_{\max}(T)} f_\gamma(E,T)\sigma(i\to j)dE + s\sum_{j\neq i} Y_j \int_{Q_{j\to i}}^{E_{\max}(T)} f_\gamma(E,T)\sigma(j\to i)dE \;, \tag{14}$$

where $\sigma(j\to i)$ is the energy-dependent cross section for photodissociation of element j to element i, with energy threshold $Q_{j\to i}$. Here we have assumed that nuclear recombination is negligible at low temperature, $T\sim 1$ keV. Equation (14) is a coupled set of differential equations for the light-element abundances. Rather than solve the full network, we can take advantage of the fact that only a few terms are important. For example, photoproduction of ^{4}He by heavier elements is negligible. As a result, the final ^{4}He abundance is given by

$$Y_4(\infty) = Y_4(t_{\rm nuc})\exp\left[-\int_{t_4}^{\tau_X}\Gamma_4(t)dt\right] \tag{15}$$

where

$$\Gamma_4(t) = s\int_{Q_4}^{E_{\max}(T)} f_\gamma(E,T)\sigma_4(E)dE \tag{16}$$

Here, $Y_4(t_{\rm nuc})$ is the ^{4}He abundance at the end of big-bang nucleosynthesis, t_4 is the time at the onset of ^{4}He dissociation, $Q_4 \simeq 20$ MeV is the photofission threshold, and σ_4 is the total cross section:

$$\sigma_4 = \sigma({}^4{\rm He}\to{}^3{\rm H}) + \sigma({}^4{\rm He}\to{}^3{\rm He}) + \sigma({}^4{\rm He}\to{\rm D}) \;. \tag{17}$$

In fact, for $m_X \gtrsim 25$ MeV, the strongest constraint arises from overproduction of the lighter elements, particularly ^{3}H+^{3}He. From Eqs. (14)–(16), the ^{3}He+^{3}H abundance at time t is given by[11]

$$Y_3(t) = \exp\left[-\int_{t_3}^{t}\Gamma_3(t')dt'\right]\left[Y_3(t_{\rm nuc}) + Y_4(t_{\rm nuc})\int_{t_4}^{t}\Gamma_{4\to 3}(t')\exp\left[-\int_{t_4}^{t'} dt''[\Gamma_4(t'')-\Gamma_3(t'')]\right]dt'\right] \;, \tag{18}$$

where $\Gamma_3(t)$, the total ^{3}He+^{3}H destruction rate, is defined analogously to Eq. (16), t_3 is the time at the onset of ^{3}He+^{3}H photodissociation, and $\Gamma_{4\to 3}$ is the part of Γ_4 that has ^{3}He and ^{3}H as end products. Since the photofission cross sections of ^{4}He, ^{3}He, and ^{3}H are comparable, their fractional destruction rates, $\dot{Y}_i/Y_i$, are of the same order of magnitude. However, since $Y_4(t_{\rm nuc}) \sim 10^4 Y_3(t_{\rm nuc})$, ^{3}H+^{3}He destruction is overwhelmed by ^{4}He$\to{}^3$He+^{3}H production for particle lifetimes $\tau_X > t_4$. Thus, even assuming *all* the initial $(t\sim t_{\rm nuc})$^{3}H+^{3}He is destroyed (since their destruction begins before that of ^{4}He), the final ^{3}He abundance will be at least

$$Y_3(\infty) \geq Y_4(\infty)\int_{t_4}^{\tau_X}\Gamma_{4\to 3}(t)dt \;. \tag{19}$$

In Eq. (19), we have implicitly included the contribution from the late ^{3}H$\to{}^3$He beta decay. From Eqs. (15) and (19), there are two regimes in which photofission limits can be obtained. If $\int_{t_4}^{\tau_X}\Gamma_4(t)dt \gtrsim 0.25$, then ^{4}He is unacceptably diluted by photofission. On the other hand, for $\int_{t_4}^{\tau_X}\Gamma_4(t)dt \ll 0.25$, ^{4}He is negligibly destroyed, $Y_4(\infty)\simeq Y_4(t_{\rm nuc})$; in this case, a strong constraint comes from the requirement that the ^{3}He abundance not exceed the observational upper bound. Note that $\sigma_{{}^4{\rm He}\to{\rm D}}$ is substantially smaller than the $4\to 3$ cross sections in Eq. (19), so no additional constraint comes from D overproduction. Also, a small additional amount of ^{3}H comes from D$+n\to{}^3$H, using neutrons from prior D dissociation; including this would only strengthen the bound coming from Eq. (19).

Using Eqs. (2), (12), (16), and (19), we find

$$\frac{Y_3(\infty)}{Y_4(\infty)} = 7.7\times 10^7 m_{\rm Pl}\frac{Y_{X,\infty}^2}{\Omega_B h^2}\int_{T_X}^{T_4} dT\langle\sigma_A|v|\rangle\frac{g_{*S}(T)}{g_*^{1/2}(T)}\int_{Q_4}^{E_{\max}(T)} dE\,\xi_\gamma(E)\frac{\sigma_{4\to 3}(E)}{\sigma_C(E)} \;. \tag{20}$$

Here $T_X = T(\tau_X)$ is the temperature when the particle decays, and T_4 is the temperature when ^{4}He photodestruction begins; it is determined by the condition $E_{\max}\simeq Q_4$, so that $T_4 \simeq 2em_e^2/25Q_4 \simeq 0.8\,e$ keV, and $t_4 \simeq (2\times 10^6/e^2)$ sec. We note that Eq. (20) is quite general and holds for any particle whose annihilations freeze out at $T\gtrsim 1$ keV.

The relevant photofission cross sections have been measured and are given in Ref. 13. To get an analytic estimate, which demonstrates how the results scale with various parameters, we approximate the total $4\to 3$ cross section by the empirical fit $\sigma({}^4{\rm He}\to{}^3{\rm He}+{}^3{\rm H}) \simeq 3.2$ mb$(E_\gamma/25\ {\rm MeV})^{-3/2} \equiv \tilde{\sigma}_4(E_\gamma/Q_{\rm eff})^{-3/2}$ (accurate to about 30% over the range $E_\gamma = 25$ to 70 MeV). Using Eqs. (13), (18), and (19), and assuming $\tau_X \gg t_4$, we obtain the approximate result

$$\frac{Y_3(\infty)}{Y_4(\infty)} \simeq \frac{2\times 10^{-9}}{(\Omega_B h^2)}\frac{\tilde{\sigma}_4}{\sigma_0}\frac{g_*(T_F)}{g_{*S}^2(T_F)}\frac{Bx_F^{2n+2}}{(n+\frac{3}{2})(n+\frac{5}{2})}\left[\frac{2em_e^2}{25Q_{\rm eff}m_X}\right]^{n+1}\frac{1}{1+2\ln(2Q_{\rm eff}/m_e)} \;, \tag{21}$$

where we have taken the slowly varying Compton logarithm out of the integral over E. For computations, we can rewrite this slightly as

$$\frac{Y_3(\infty)}{Y_4(\infty)} \simeq \frac{63}{(\Omega_B h^2)} \left[\frac{10^{-38}\ \mathrm{cm}^2}{\sigma_0}\right] \frac{g_*(T_F)}{g_{*S}^2(T_F)} \frac{B}{(n+\frac{3}{2})(n+\frac{5}{2})} \left[8.4\times 10^{-4} e x_F^2 \left[\frac{\mathrm{MeV}}{m_X}\right]\right]^{n+1} . \tag{22}$$

The determinations of the ^{3}He abundance in carbonaceous chondrites, gas-rich meteorites, and lunar soil are consistent with a presolar value for the sum of D and ^{3}He of[14] $[(\mathrm{D}+{}^3\mathrm{He})/\mathrm{H}] \simeq (3.6\pm 0.6)\times 10^{-5}$. ^{3}He is difficult to destroy in stars without also producing large amounts of ^{4}He or heavy elements. If we conservatively assume that ^{3}He can have astrated (been reduced by stellar processing) by no more than a factor of 4, then we find

$$\frac{^3\mathrm{He}}{\mathrm{H}} \le \frac{^3\mathrm{He}+\mathrm{D}}{\mathrm{H}} \le 1.7\times 10^{-4} . \tag{23}$$

Since the observed abundance of ^{4}He is approximately $^4\mathrm{He}/\mathrm{H}=0.07$, this yields the upper limit

$$\frac{Y_3(\infty)}{Y_4(\infty)} = \frac{^3\mathrm{He}}{^4\mathrm{He}} \le 2.4\times 10^{-3} . \tag{24}$$

Combining Eqs. (22) and (24), we find a constraint on the particle mass:

$$\frac{m_X}{\mathrm{MeV}} \ge 8.4\times 10^{-3} e x_F^2 \left[\frac{2.6\times 10^4 B}{g_*(T_F)\Omega_B h^2 (n+\frac{3}{2})(n+\frac{5}{2})} \left[\frac{10^{-38}\ \mathrm{cm}^2}{\sigma_0}\right]\right]^{1/(n+1)} . \tag{25}$$

[Here, we have assumed that freeze-out occurs before electron-positron annihilation, $T_F \gtrsim 0.5$ MeV, so that $g_*(T_F)=g_{*S}(T_F)$.] This expression can be simplified for two important cases: For $n=0$, i.e., if the annihilation cross section is independent of temperature, we have

$$\left[\frac{m_X}{\mathrm{MeV}}\right]_{n=0} \ge 1.8\times 10^4 Be \left[\frac{x_F}{10}\right]^2 \left[\frac{10.75}{g_*(T_F)}\right] \left[\frac{0.03}{\Omega_B h^2}\right] \left[\frac{10^{-38}\ \mathrm{cm}^2}{\sigma_0}\right] , \tag{26}$$

while for $n=1$ we obtain

$$\left[\frac{m_X}{\mathrm{MeV}}\right]_{n=1} \ge 80 B^{1/2} e \left[\frac{x_F}{10}\right]^2 \left[\frac{10.75}{g_*(T_F)} \frac{0.03}{\Omega_B h^2} \frac{10^{-38}\ \mathrm{cm}^2}{\sigma_0}\right]^{1/2} . \tag{27}$$

The actual numerical mass limit will depend on T_F and the cross section σ_0 (which in turn is usually a function of m_X). We discuss a few examples in the next section.

Now, ^{4}He photodestruction begins and peaks rapidly at $t_4 = 2\times 10^6\, e^{-2}$ sec, so the mass limits above apply to particles with lifetimes $\tau_X > t_4$ and masses $m_X > Q_4 = 20$ MeV. We should make one remark about this mass range. At the low-mass end $m_X \sim Q_4$ the double-photon cutoff $E_{\max}(T)$ becomes comparable to the primary photon energy m_X soon after $t \simeq t_4$. At later times, double-photon scattering is irrelevant, and the shower spectrum evolution must be treated differently.[3,15] Although this may be expected to change the low-mass results somewhat, this is mitigated by the fact that the ^{4}He photofission rate peaks very near "turn-on" at t_4. Consequently, the photofission yields at the low-mass end decrease by less than a factor of 2 at the relevant temperatures,[8] and our bound applies.

For particle masses less than 20 MeV, other photofission processes play an important role. In this case, the dominant reactions are $^7\mathrm{Li}(\gamma,T)^4\mathrm{He}$ ($Q_7=2.5$ MeV), ^{3}He destruction ($Q_3=5.5$ MeV), and $\mathrm{D}(\gamma,n)p$ ($Q_2=2.2$ MeV). These destruction processes compete with, e.g., D production from $^3\mathrm{He}(\gamma,p)\mathrm{D}$ and $^3\mathrm{H}(\gamma,n)\mathrm{D}$, and neutron capture on D to form ^{3}H (using neutrons from D destruction). The most straightforward bound comes from ^{7}Li destruction through (γ,T), (γ,p), and (γ,n), with the constraint (assuming the ^{7}Be photofission cross section is roughly equal to that of ^{7}Li)

$$Y_7(\infty) = Y_7(t_{\mathrm{nuc}}) \exp\left[-\int_{t_7}^{\tau_X} \Gamma_7(t)\,dt\right] > \min(Y_7^{\mathrm{observed}}) . \tag{28}$$

The general expression for $\int \Gamma_7 dt$ is found from Eq. (20) by making the replacements $T_4, Q_4, \sigma_{4\to 3} \to T_7, Q_7, \sigma_7$. Although experimental results show some scatter,[16] the $^7\mathrm{Li}(\gamma,T)^4\mathrm{He}$ photofission cross section is characterized by a threshold at $E_\gamma = 2.5$ MeV, a peak with $\sigma_7 \simeq 0.5$ mb at $E_\gamma \simeq 7$ to 10 MeV, and $\sigma_7 \simeq 0.2$ mb for $E_\gamma \simeq 11$ to 15 MeV, followed by a gradual falloff at higher energies.[16] Considering only the range $E_\gamma = 7$ to 10 MeV, we find, analogously to Eq. (21),

$$\int_{t_7} \Gamma_7(t)\,dt = \frac{2\times 10^{-9}}{\Omega_B h^2} \frac{\tilde{\sigma}_7}{\sigma_0} \frac{g_*(T_F)}{g_{*S}^2(T_F)} \frac{B x_F^{2n+2}}{1+2\ln(2Q_7/m_e)} \left[\frac{2em_e^2}{25 Q_7 m_X}\right]^{n+1}$$
$$\times \frac{1-2(Q_7/\tilde{E}_m)^{n+1}[n+\frac{3}{2}-(n+1)(Q_7/\tilde{E}_m)^{1/2}]}{(n+1)(n+\frac{3}{2})} , \tag{29}$$

where $Q_7=7$ MeV, $\tilde{E}_m=10$ MeV, and $\tilde{\sigma}_7=0.5$ mb.

In standard big-bang nucleosynthesis, the maximum ^{7}Li/H fraction produced is less than or equal to 10^{-9} (assuming $10^{-10}<\eta<10^{-9}$), while the ^{7}Li/H abundance in low metallicity halo and old disk dwarfs is greater than[17] 5×10^{-11}. Thus, even being very conservative, we can only tolerate a ^{7}Li depletion factor of 20. From Eq. (28) this implies the constraint $\int\Gamma_7 dt<3$; using Eq. (29), this gives, for $n=0$,

$$\left[\frac{m_X}{\text{MeV}}\right]_{n=0}\geq 2.1Be\left[\frac{x_F}{10}\right]^2\frac{g_*(T_F)}{g_{*S}^2(T_F)}\left[\frac{0.03}{\Omega_B h^2}\right]\left[\frac{10^{-38}\text{ cm}^2}{\sigma_0}\right] \tag{30}$$

and, for $n=1$,

$$\left[\frac{m_X}{\text{MeV}}\right]_{n=1}\geq 0.7B^{1/2}e\left[\frac{x_F}{10}\right]^2\left[\frac{g_*(T_F)}{g_{*S}^2(T_F)}\frac{0.03}{\Omega_B h^2}\frac{10^{-38}\text{ cm}^2}{\sigma_0}\right]^{1/2} . \tag{31}$$

The results discussed so far are quite general and can be applied to a wide class of particle-physics models. As an application, we consider a specific model below.

IV. APPLICATIONS

We can use the photofission results above to derive constraints on the mass and lifetime of long-lived particles. Such candidate particles include, for example, the tau neutrino and the lightest supersymmetric particle (LSP). (In the latter case, for LSP masses in the range we consider, $m_X<1$ GeV, R parity must be broken so that the LSP can decay.) In this section, as a worked example we consider a massive Dirac neutrino.

For a Dirac-neutrino species, the annihilation cross section is approximately $\sigma_0\simeq 5m_\nu^2G_F^2/2\pi$, with the s wave dominating ($n=0$). The electromagnetic branching ratio for neutrino annihilations is $B\simeq\frac{1}{2}$, and the freeze-out epoch is $x_F\simeq 17.7+3\ln(m_\nu/\text{GeV})$. For a mass of the order of 1 GeV, we have $T_F\simeq 56$ MeV, so that $g_*(T_F)=g_{*S}(T_F)=10.75$. In this case, Eq. (21) yields

$$\frac{Y_3(\infty)}{Y_4(\infty)}\simeq 1.6\times10^{-3}\left[\frac{\Omega_B h^2}{0.03}\right]^{-1}\left[\frac{m_\nu}{\text{GeV}}\right]^{-3}e \tag{32}$$

from which we obtain the bound $m_\nu\geq 1.0\,e^{1/3}$ GeV. We have thus found that Dirac neutrinos with mass 20 MeV $\lesssim m_\nu\lesssim 1.0\,e^{1/3}$ GeV must have lifetimes $\tau_\nu\lesssim 2\times10^6$ e^{-2} sec in order not to overproduce ^{3}He. Here, the lower mass limit comes from the requirement $m_\nu>Q_4$. We emphasize that this bound holds even if the neutrino does not decay radiatively. (Note that for $m_\nu\lesssim 1$ GeV, we need not consider baryonic annihilation products.) These results are shown as the excluded region C in Fig. 1, in a plot of lifetime τ_ν vs neutrino mass m_ν.

For neutrinos lighter than 20 MeV, we consider the bound from ^{7}Li destruction. Using Eq. (30), for a Dirac neutrino the ^{7}Li depletion is given by

$$\ln\left[\frac{Y_7(t_{\text{nuc}})}{Y_7(\infty)}\right]\simeq 6\times10^{-5}\left[\frac{\Omega_B h^2}{0.03}\right]^{-1}\left[\frac{m_\nu}{\text{GeV}}\right]^{-3}e \tag{33}$$

for $\tau_\nu>t_7\simeq 10^5e^{-2}$ sec. The constraint that $Y_7(t_{\text{nuc}})/Y_7(\infty)<20$ implies the bound

$$m_\nu\geq 27\text{ MeV}e^{1/3}\left[\frac{\Omega_B h^2}{0.03}\right]^{-1/3} \tag{34}$$

to avoid overdepletion of ^{7}Li. Thus Dirac neutrinos in the mass range 7 MeV $\lesssim m_\nu\lesssim 25$ MeV must have a lifetime $\tau_\nu\lesssim(1$ to $4)\times10^5$ sec. The disallowed range is shown as region D in Fig. 1.

There are two additional bounds which, although independent of the photofission constraint above, overlap them in the mass versus lifetime plane. The first additional constraints comes from the fact that the X particle energy density *during* big-bang nucleosynthesis can alter the light element abundances, in particular increasing D and ^{4}He.[18] As a result, particles with mass in the range $m_X\simeq 0.5$ to 10 MeV must have a lifetime $\tau_X\lesssim 1$ sec or so.[18] This bound is shown in Fig. 1 as region B. Second, there is the requirement that the present energy density

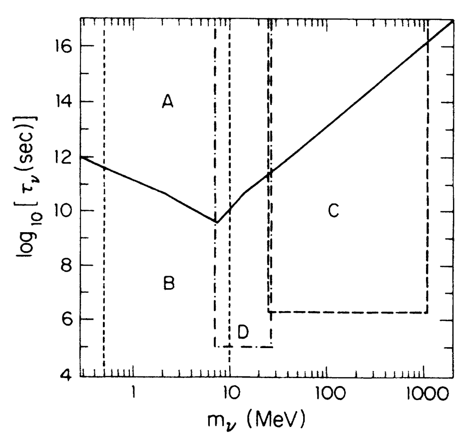

FIG. 1. Forbidden regions of the mass-lifetime plane for a Dirac-neutrino species. The region interior to the solid curve (A) is forbidden by requiring that $\Omega_\nu h^2\lesssim 1$. Region B is ruled out due to the effects of the neutrino energy density *during* nucleosynthesis. Regions C and D are forbidden based upon the photodissociation of the light elements triggered by eternal annihilations, in particular ^{4}He (C) and ^{7}Li (D).

of particle decay products is not too large, $\Omega_X h^2 \leq 1$. The resulting forbidden region of mass and lifetime[1,9] is marked A in Fig. 1. (Requiring the Universe to become matter dominated "on schedule," so that structure formation can proceed in the usual way, yields a stronger bound.) We note that, as with the photofission bounds above, these constraints are independent of decay channel.

V. CONCLUSION

While the annihilations of a massive, weakly interacting relic species cease to significantly decrease the number of relics per comoving volume after "freeze-out," i.e., for $T \lesssim T_F$ where $\Gamma_A(T_F) \simeq H(T_F)$, annihilations do continue eternally. Annihilations that take place around 10^5 to 10^6 sec after the big bang can significantly alter the primordial abundances of D, ^{4}He, and especially ^{3}He and ^{7}Li. Using this fact, we have derived stringent new constraints that apply to a massive particle species with roughly weak interactions and lifetime greater than about 10^4 sec. Unlike many previous bounds, these apply irrespective of the decay mode of the species. As an example, we have applied our constraints to a Dirac-neutrino species, and have ruled out lifetimes greater than about 10^5 to 10^6 sec for masses between 10 and 1000 MeV.

ACKNOWLEDGMENTS

We thank S. Dodelson and J. Hagelin for useful conversations. This work was supported in part by the U.S. Department of Energy (DOE) and by NASA (Grant NAGW-1340) at Fermilab, and by the DOE at Chicago.

[1] D. A. Dicus, E. W. Kolb, and V. L. Teplitz, Phys. Rev. Lett. **39**, 168 (1977).

[2] B. Lee and S. Weinberg, Phys. Rev. Lett. **39**, 165 (1977); S. Gershtein and Ya. B. Zeldovich, Pis'ma Zh. Eksp. Teor. Fiz. **4**, 174 (1966) [JETP Lett. **4**, 120 (1966)]; R. Cowsik and J. McCleland, Phys. Rev. Lett. **29**, 669 (1972); A. Szalay and G. Marx, in *Neutrino '72*, proceedings of the Europhysics Conference, Balatonfured, Hungary, 1972, edited by A. Frenkel and G. Marx (OMKD-Technoinform, Budapest, 1972).

[3] D. Lindley, Mon. Not. R. Astron. Soc. **188**, 15 (1979); Astrophys. J. **294**, 1 (1985); J. Audouze, D. Lindley, and J. Silk, *ibid.* **293**, L53 (1985).

[4] See, e.g., N. Terasawa, M. Kawasaki, and K. Sato, Nucl. Phys. **B302**, 697 (1988), and references therein.

[5] G. Gelmini and M. Roncadelli, Phys. Lett. **99B**, 411 (1981); Y. Chikashige, R. Mohapatra, and R. Peccei, *ibid.* **98B**, 265 (1981).

[6] G. Gelmini and J. Valle, Phys. Lett. **142B**, 181 (1984); J. Schechter and J. Valle, Phys. Rev. D **25**, 774 (1982); J. Valle, Phys. Lett. **131B**, 87 (1983).

[7] J. Frieman and G. Giudice, Phys. Lett. B **224**, 125 (1989).

[8] J. Hagelin and R. Parker (unpublished); J. Hagelin, R. Parker, and A. Honberg, Phys. Lett. B **215**, 397 (1988); M. H. Reno and D. Seckel, Phys. Rev. D **38**, 3441 (1988).

[9] See, e.g., E. W. Kolb and M. S. Turner, *The Early Universe* (Addison-Wesley, Redwood City, CA, 1989), Chap. 5.

[10] M. Kawasaki, N. Terasawa, and K. Sato, Phys. Lett. B **178**, 71 (1986).

[11] S. Dimopoulos, R. Esmailzadeh, L. Hall, and G. Starkman, Phys. Rev. Lett. **60**, 7 (1988); Astrophys. J. **330**, 545 (1988); Nucl. Phys. **B311**, 699 (1988).

[12] F. Aharonian and V. Vardanian, Yerevan Physics Institute report, 1985 (unpublished); M. Burns and R. Lovelace, Astrophys. J. **262**, 87 (1982).

[13] Yu. M. Arkatov *et al.*, Yad. Fiz. **12**, 227 (1970) [Sov. J. Nucl. Phys. **12**, 123 (1971)]; A. Gorbunov and V. Spiridonov, Zh. Eksp. Teor. Fiz. **34**, 866 (1958) [Sov. Phys. JETP **7**, 600 (1958)]; Yu. M. Arkatov *et al.*, Pis'ma Zh. Eksp. Teor. Fiz. **24**, 478 (1976) [JETP Lett. **24**, 440 (1976)]; Yu. M. Arkatov *et al.*, Yad. Fiz. **19**, 1172 (1974) [Sov. J. Nucl. Phys. **19**, 598 (1974)].

[14] J. Yang *et al.*, Astrophys. J. **281**, 493 (1984).

[15] G. R. Blumenthal and R. J. Gould, Rev. Mod. Phys. **42**, 237 (1970).

[16] D. M. Shopik *et al.*, Phys. Rev. C **20**, 2025 (1979); G. Junghaus *et al.*, Z. Phys. A **291**, 353 (1979); V. P. Denisov and I. Chubakov, Yad. Fiz. **35**, 11 (1982) [Sov. J. Nucl. Phys. **35**, 6 (1982)].

[17] F. Spite and M. Spite, Astron. Astrophys. **115**, 357 (1982); F. Spite, J. P. Maillard, and M. Spite, *ibid.* **141**, 56 (1984).

[18] E. W. Kolb and R. Scherrer, Phys. Rev. D **25**, 1481 (1982).